Model for a photoinduced insulator-metal transition in a one-dimensional quarter-filled organic salt: Evidence for a nonadiabatic charge-phonon coupling

J. D. Lee
School of Materials Science, Japan Advanced Institute of Science and Technology, Ishikawa 923-1292, Japan
(Received 5 August 2009; published 1 October 2009)

We study the photoinduced nonequilibrium dynamics of a one-dimensional quarter-filled organic salt. Cooperative onsets of charge-order melting and coherent phonon generation are found in the early stage to $\tau \sim \tau_{ex}$ (where τ_{ex}: the pulse length of the pumping laser), which signifies that they are mutually driven. Later, at $\tau \gtrsim \tau_{ex}$, there is nonadiabatic decoupling of the charge-order melting and coherent phonon generation. Calculation of optical conductivity and time-resolved photoemission spectra at $\tau \gtrsim \tau_{ex}$ is consistent with the recent experimental observations, which confirms a nonadiabatic charge-phonon interaction in the ultrafast time span.

DOI: 10.1103/PhysRevB.80.165101 PACS number(s): 78.66.Qn, 63.20.kd, 78.20.Bh, 78.47.−p

I. INTRODUCTION

Novel optically driven transient changes in electronic, magnetic, and lattice structures incorporating an instability due to cooperative interaction among corresponding degrees of freedom are classified as photoinduced phase transitions (PIPTs).[1–4] Insulator-metal transition (IMT), one of the most intriguing phenomena in condensed-matter physics,[5] can be also triggered by the simultaneous introduction of electron and hole through the photoirradiation of an insulator. The photoinduced insulator-metal transition (PIIMT) may be categorized depending on whether or not it accompanies the structural changes. One-dimensional (1D) halogen-bridged Ni complex, known as the Mott insulator, undergoes PIIMT without structural changes.[6–8] There are broader classes of examples for which PIIMT accompanies the structural changes in a cooperative manner through ultrafast charge-lattice-coupled dynamics after photoexcitation.[1–4]

The 1D quarter-filled (with holes; three quarter filled with electrons) organic salt $(EDO\text{-}TTF)_2PF_6$(EDO-TTF =ethylenedioxy-tetrathiafulvalene) shows IMT from the low-temperature (LT) phase of the (0110) charge order (CO) to a high-temperature (HT) metallic phase,[9,10] where (0110) represents an array of neutral and ionic EDO-TTF molecules (D); i.e., $D^0D^+D^+D^0$. T_C is 278 K for $(EDO\text{-}TTF)_2PF_6$. The observed photoresponses together with the PIIMT originate presumably from the underlying electron-phonon interaction. However, a proper understanding of the driving forces of such photoresponses in the femtosecond time range is still unclear. Intriguingly, in a system with strong electron-phonon coupling, the ultrafast dynamics show unexpected nonadiabatic behaviors of electrons and phonons depending on the photoexcitation conditions,[3,11] which differs from the case of a standard solid for which the electrons obey the Born-Oppenheimer approximation (BOA).[12] This nonadiabatic behavior might be an essential criterion for cooperative PIPT induced by ultrafast charge-lattice-coupled dynamics.[3]

In this paper, we investigate the underlying dynamics of charge and phonon in PIIMT for $(EDO\text{-}TTF)_2PF_6$. Two kinds of phonons are considered to obtain the correct ground state of the (0110) CO to which two kinds of orders (bond and charge orders) are attributed.[13] General nonadiabatic interaction between charge and phonon is explored by treating both within a single-quantum-mechanical framework. We find that the cooperative onset of CO melting and coherent phonon generation occurs in $\tau \lesssim \tau_{ex}$ (where τ_{ex} is the pulse length of the pumping laser). This implies that they could be driving forces for each other. Later, at $\tau \gtrsim \tau_{ex}$, there is the photoinduced decoupling of the interaction between them, which is a purely nonadiabatic feature. Our study of optical conductivity and time-resolved photoemission spectra (TRPES) at $\tau \gtrsim \tau_{ex}$ shows a reasonable agreement with the recent experimental observations. This gives an evidence for the importance of a nonadiabatic charge-phonon coupling of the system in the ultrafast time span.

The paper is organized as follows. In Sec. II, we give a model of the system and describe the formulation. In Sec. III, we discuss the results of the study in three different directions: (i) the nonadiabatic decoupling between charge density and coherent phonon oscillation, (ii) the optical conductivity, and (iii) the time-resolved photoemission. Finally, in Sec. IV, we provide a summary and conclusion.

II. MODEL AND FORMULATION

We consider that interacting holes by the Hubbard U on a 1D chain are coupled with two different kinds of phonons. The resulting Hamiltonian $\mathcal{H}_0$ is a Peierls-Holstein-Hubbard-type one.[14] Combining $\mathcal{H}_0$ with the light-matter interaction, the total Hamiltonian $\mathcal{H}(=\mathcal{H}_0+\mathcal{V})$ reads

$$\mathcal{H}_0 = t\sum_{i\sigma}[1 - g_\alpha(b^\dagger_{i\alpha} + b_{i\alpha} - b^\dagger_{i+1\alpha} - b_{i+1\alpha})] \times (c^\dagger_{i\sigma}c_{i+1\sigma} + c^\dagger_{i+1\sigma}c_{i\sigma}) + U\sum_i n_{i\uparrow}n_{i\downarrow} - g_\beta\sum_{i\sigma}(b^\dagger_{i\beta} + b_{i\beta})c^\dagger_{i\sigma}c_{i\sigma} + \omega_\alpha\sum_i b^\dagger_{i\alpha}b_{i\alpha} + \omega_\beta\sum_i b^\dagger_{i\beta}b_{i\beta},$$

$$\mathcal{V} = \hat{j}A_{ex}e^{i\omega_{ex}\tau}\bar{\Theta}(\tau) + \text{H.c.}, \quad (1)$$

where $c^\dagger_{i\sigma}(c_{i\sigma})$ is the operator of a hole with spin σ at site i (i.e., at the site of the EDO-TTF molecule) and $n_{i\sigma}$ is the number operator of the hole, given by $n_{i\sigma}=c^\dagger_{i\sigma}c_{i\sigma}$. t is the

hopping parameter and U the on-site Coulomb repulsion. $b_{i\alpha}^{\dagger}(b_{i\alpha})$ and $b_{i\beta}^{\dagger}(b_{i\beta})$ are operators for two different kinds of phonons, α and β, the energies of which are ω_{α} and ω_{β}, respectively. The ionic displacement $u_i^{\alpha(\beta)}$ is proportional to $b_{i\alpha(\beta)}^{\dagger}+b_{i\alpha(\beta)}$ for each phonon. According to $\mathcal{H}_0$, for the α phonon, $u_i^{\alpha}-u_{i+1}^{\alpha}$ couples with the bond strength while for the β phonon, u_i^{β} couples with the hole charge density. g_{α} and g_{β} are the hole-phonon coupling constants for the α and β phonons. $\mathcal{V}$ is the light-matter interaction due to the optical pumping pulse. Its field strength and energy are A_{ex} and ω_{ex}, respectively. $\bar{\Theta}(\tau)$ simulates the pulse shape, $\bar{\Theta}(\tau)=\Theta(\tau)-\Theta(\tau-\tau_{\mathrm{ex}})$. $\Theta(\tau)$ is the Heaviside step function. Finally, $\hat{j}$ is the current operator expressed as $\hat{j}=it\Sigma_{i\sigma}(c_{i+1\sigma}^{\dagger}c_{i\sigma}-c_{i\sigma}^{\dagger}c_{i+1\sigma})$.

Exact diagonalization using the Lanczos method with $N=8$ (where N is the number of sites; i.e., $N/2$ holes are introduced) gives the many-body ground state $|\Psi(0)\rangle$. The Hilbert space necessary for the Lanczos method would be written as $\Pi_i|\psi_i^l\rangle\otimes\Pi_{i'}|n_{i'}^{\alpha}\rangle\otimes\Pi_{i''}|n_{i''}^{\beta}\rangle$. $|\psi_i^l\rangle$ is the hole state at site i; i.e., $|0\rangle$, $|\uparrow\rangle$, $|\downarrow\rangle$, and $|\uparrow\downarrow\rangle$ according to $l=0$, 1, 2, and 3, respectively. $|n_{i'}^{\alpha}\rangle$ and $|n_{i''}^{\beta}\rangle$ are the phonon states with phonon numbers $n_{i'}^{\alpha}$ and $n_{i''}^{\beta}(=0,1,2,\ldots)$ at sites i' and i'', respectively. Here, we simplify the Hilbert space by cutting the phonon number hierarchy and restricting the phonon numbers to only 0 or 1 per mode and per site.[15] The adopted parameters for a given charge-phonon-coupled system are $U=1.5$, $g_{\alpha}=0.5$, $g_{\beta}=0.01$, $\omega_{\alpha}=0.01$, and $\omega_{\beta}=0.05$ unless stated otherwise. All energy quantities are given in a unit of t. We find the ground-state charge density $\langle\Sigma_{\sigma}c_{i\sigma}^{\dagger}c_{i\sigma}\rangle$ from $\langle\Psi(0)|\Sigma_{\sigma}c_{i\sigma}^{\dagger}c_{i\sigma}|\Psi(0)\rangle$ to be 0.36, 0.64, 0.64, and 0.36 at sites $i=0$, 1, 2, and 3 repeating with four-site periodicity. This reproduces the LT phase of the (0110) CO observed in $(EDO\text{-}TTF)_2PF_6$.[16] In the same way, the static phonon amplitudes are calculated. We find $\langle b_{i\alpha}^{\dagger}+b_{i\alpha}\rangle$ to be −0.56, −0.56, 0.56, and 0.56 at sites $i=0$, 1, 2, and 3 with four-site periodicity, which gives a bond order of $D^0-D^+=D^+-D^0$ (where "=" indicates a strong bond and "–" a weak bond). β phonons are coupled to the charge density so that their distortions relate to the (0110) CO. That is, with the same periodicity, values of $\langle b_{i\beta}^{\dagger}+b_{i\beta}\rangle$ are −0.12, 0.12, 0.12, and −0.12 at sites $i=0$, 1, 2, and 3.

In $(EDO\text{-}TTF)_2PF_6$, as shown in our calculation, the (0110) CO [called bond-charge-density wave (BCDW)] is stabilized by two types of phonons, i.e., transfer-integral-modulating displacement [the first term of Eq. (1)] and the site-energy-modulating deformation [the third term of Eq. (1)]. According to the extended study on the 1D quarter-filled itinerant charges coupled to classical phonons, the BCDW is found to compete with the (1010) charge-density wave (CDW) spin-Peierls (SP) state at LT.[13] However, for $(EDO\text{-}TTF)_2PF_6$, Drozdova *et al.*[17] confirm that almost all charge density is localized on the strongly bound central pair of (0110) tetramer. It is also interesting to compare the present phase with various charge-phonon-coupled phases in other 1D organic compounds. The mixed-stack organic charge-transfer (CT) complex, TTF-CA (=tetrathiafulvalene-p-chloranil), shows the PIPT from the ionic to neutral state by the photoexcitation.[18] This would be described by the 1D half-filled extended Peierls-Hubbard model.[19] In the ionic state, molecules are dimerized due to the SP mechanism, which implies that the charge-phonon interaction leading to the renormalized Coulomb interaction due to the bond deformation is crucial in the PIPT. Another PIPT accompanying the structural changes would be the transition from the CDW to the Mott insulator, which is observed in the 1D Br-bridged Pd-chain compound, $[Pd(chxn)_2Br]Br_2$(chxn =cyclohexanediamine).[20] This would be described by the model similar to the TTF-CA but alternating Pd $4d_{z^2}$ and Br $4p_z$ orbitals should be taken into account.[21] In the sense, the relevant model would be called the *dp* model. For various examples and detailed discussion, see, for example, Ref. 1.

With the Lanczos ground state $|\Psi(0)\rangle$, we solve the time-dependent Schrödinger equation in the nonperturbative many-body time-dependent approach.[7,22] The time evolution of $|\psi(\tau)\rangle$ should be done within the same many-body Hilbert space as used for the Lanczos diagonalization. We can write the quantum state of the whole system at time τ as $|\Psi(\tau)\rangle=\Sigma_{\{l,n^{\alpha},n^{\beta}\}}C_{\{l,n^{\alpha},n^{\beta}\}}(\tau)|\{l,n^{\alpha},n^{\beta}\}\rangle$. $|\{l,n^{\alpha},n^{\beta}\}\rangle$ corresponds to $\Pi_i|\psi_i^l\rangle\Pi_{i'}|n_{i'}^{\alpha}\rangle\Pi_{i''}|n_{i''}^{\beta}\rangle$. Dynamics that begin with the turning on of the optical pumping at $\tau=0$ can then be described by solving the coupled differential equations for $C_{\{l,n^{\alpha},n^{\beta}\}}(\tau)$ resulting from the time-dependent Schrödinger equation $i\partial/\partial\tau|\Psi(\tau)\rangle=\mathcal{H}|\Psi(\tau)\rangle$. The initial condition $|\Psi(0)\rangle$ should be the ground state. We treat the charge-phonon-coupled chain of $N=8$ (i.e., four holes) with the periodic boundary condition imposed.

III. RESULTS

A. Nonadiabatic decoupling of charge density and coherent phonon oscillation

Figures 1 and 2 illustrate the dynamics of charges and local phonons (β phonons) at sites $i=0$, 1, 2, and 3 with respect to the field strength A_{ex} or the pulse length τ_{ex}. The dynamics begin at $|\Psi(0)\rangle$ with the switching on of the optical pumping laser. Time is given in a unit of $1/t$. For instance, if taking $t=0.2$ eV, $1/t$ corresponds to 3.3 fs. Figure 1 shows the early dynamics just after photoexcitation. It shows the simultaneous onset of CO (or collapse) and coherent phonon generation. In Fig. 1(a) with $\tau_{\mathrm{ex}}=30$, for $A_{\mathrm{ex}}=0.5$, CO melting is not complete and coherent phonon oscillation is not fully relaxed. For higher A_{ex}, however, there is complete melting of the CO and full relaxation of coherent phonons within $\sim\tau_{\mathrm{ex}}$. This incorporates the coherent and cooperative interplay between charges and phonons in the early stage to $\tau\sim\tau_{\mathrm{ex}}$. Such interplay during photoirradiation is further confirmed by comparing the dynamics of $\tau_{\mathrm{ex}}=30$ [second panel of Fig. 1(a)] with those of $\tau_{\mathrm{ex}}=10$ [Fig. 1(b)] for a fixed value of $A_{\mathrm{ex}}=1$. Dynamics for a shorter photoirradiation time ($\tau_{\mathrm{ex}}=10$) cannot fully induce CO melting and coherent phonon generation. On the other hand, as shown in Fig. 2, considering the long timespan of $\tau\gtrsim\tau_{\mathrm{ex}}$, we do not find any phonon-related dynamical scale in the time-dependent behavior of the charges. This is interesting because it sharply contrasts with the dynamics of charge degrees of freedom under the adiabatic potential based on the

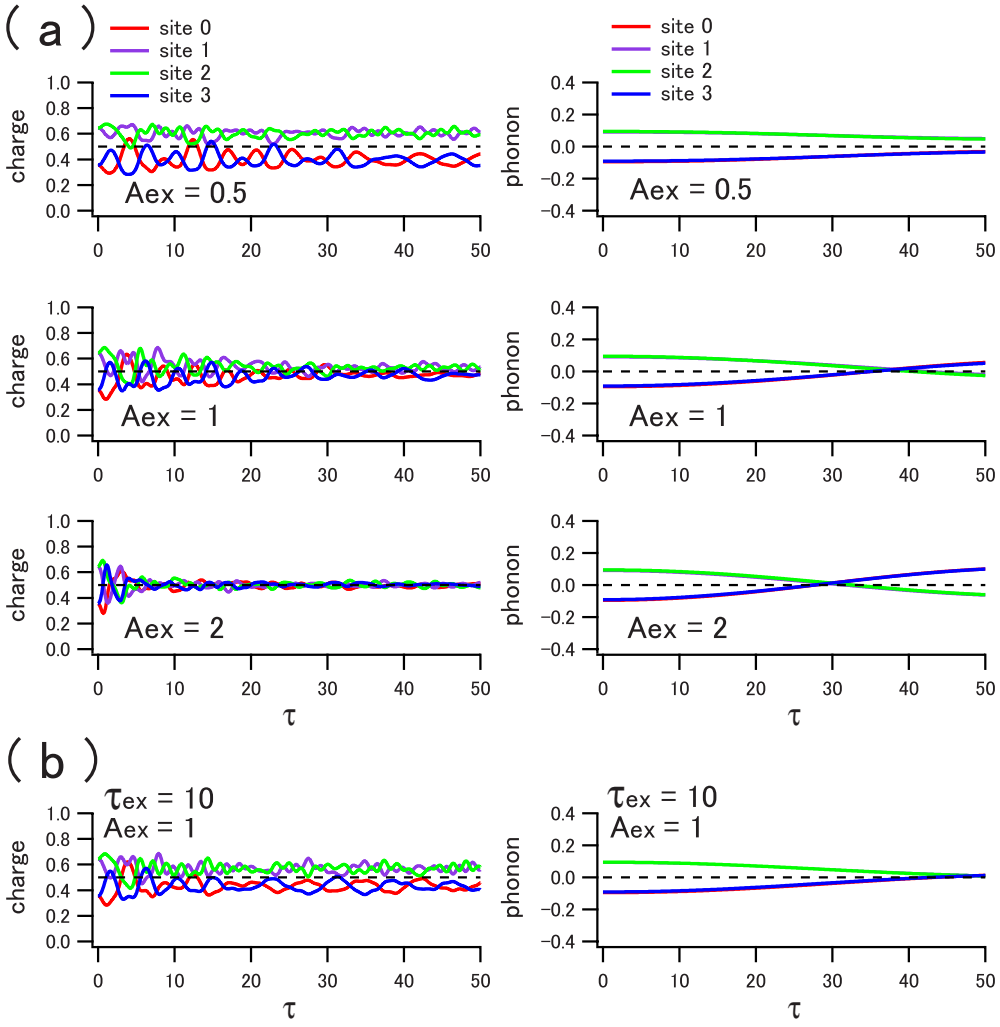

FIG. 1. (Color online) Dynamics of charges and local phonons (β phonons); i.e., $\langle \Sigma_\sigma c_{i\sigma}^\dagger c_{i\sigma} \rangle$ and $\langle b_{i\beta}^\dagger + b_{i\beta} \rangle$ at molecular sites $i=0$, 1, 2, and 3 on a 1D chain with respect to parameters of the optical pumping laser. Quantities of energy and time are given in units of t and $1/t$, respectively. (a) Dynamics with respect to the field strength A_{ex} for $\tau_{ex}=30$. (b) Dynamics with $\tau_{ex}=10$ and $A_{ex}=1$. Both (a) and (b) adopt $\omega_{ex}=1.5$.

BOA.[12] In fact, if considering the BOA, the charge system reacts instantly to the lattice configuration so that its dynamics should incorporate characteristic time scales of the lattice motion.[10,23] Remembering that we handle charge and phonon in a single-quantum-mechanical framework without taking the BOA, we find that the dynamics in the long time range of $\tau \gtrsim \tau_{ex}$ in Fig. 2 signify the photoinduced decoupling between charge density and phonon oscillation, which would be a purely nonadiabatic feature.[3,11]

Interestingly, for the weak-field intensity of the pump pulse, the dynamics of charge density are found to undergo the nonadiabatic-adiabatic transition. In Fig. 3, the temporal motion of the charge density at the site 1 is displayed. For $A_{ex}=0.25$, we clearly find that the dynamics incorporate the time scale of the phonon, i.e., the charge density oscillates with $\sim 2\omega_\beta$. This means that the charge and phonon move adiabatically for weaker field intensities, consistent with the recent experiment on the electronic conductivity of VO_2 decoupled from the coherent lattice motion.[3] However, for the weak-field intensity of $A_{ex}=0.25$, the charge density at the site 1 starting from 0.64 at $\tau=0$ hardly changes as τ elapses in an average sense, that is, the CO hardly melts. The minimum field intensity would be necessary to obtain the PIIMT. Incidentally, for a situation clearly undergoing the PIIMT, it need be considered that the nonadiabatic charge-phonon coupling would be important.

B. Optical conductivity

Metallic nature associated with coherent phonon generation due to ultrashort laser excitation can be probed from optical transport measurements. The reflectivity[9] or optical conductivity[10] before and after the photoexcitation has been argued to monitor the metallic nature of $(EDO\text{-}TTF)_2PF_6$. In the present study, the time-dependent current $J(\tau)$ is calculated from the solution of the time-dependent Schrödinger equation; i.e., $J(\tau)=\langle \Psi(\tau)|\hat{j}|\Psi(\tau)\rangle$. Here, the optical conductivity $\sigma(\omega)$ is obtained from the Fourier transformation,

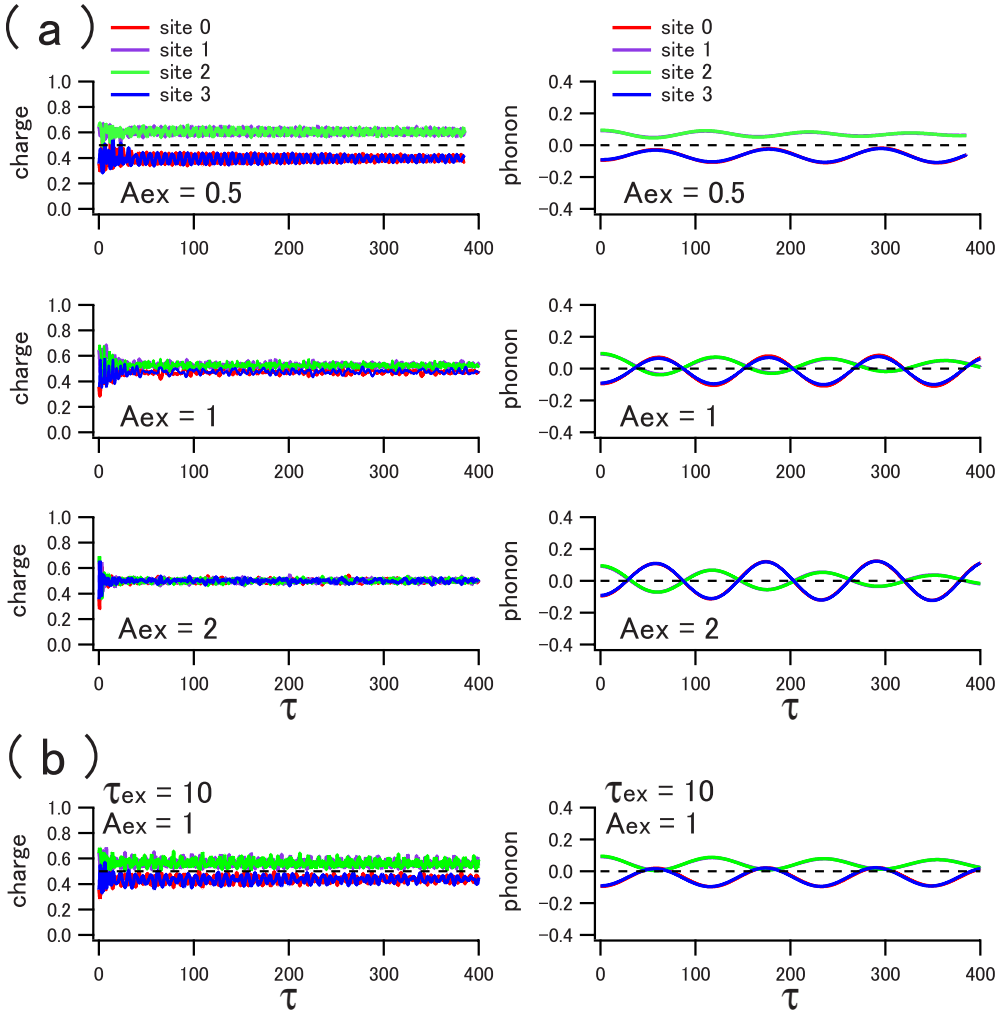

FIG. 2. (Color online) Same as in Fig. 1 but up to the long-time region.

$$\sigma(\omega) = \int_{\tau_{ex}}^{\tau_{cutoff}} d\tau e^{i\omega\tau} J(\tau), \tag{2}$$

where τ_{cutoff} is practically arbitrary in the calculation and taken to be 120. In Fig. 4, the optical conductivity $\sigma(\omega)$ after photoexcitation (in fact, the photoresponse during $\tau_{ex} < \tau < \tau_{cutoff}$) is presented with respect to the field strength A_{ex}. There are two observed distinct CT bands in the optical conductivity. One band (CT1) near 0.9 corresponds to excitation from (0110) to (1010) and the other band (CT2) near 3.9 from (0110) to (0200); i.e., $D^+D^+ \rightarrow D^{2+}D^0$. In particular, the CT2 band directly reflects the presence of CO so that a decrease in its strength with increasing A_{ex} indicates CO melting (i.e., a metallic nature), which is clearly displayed in the inset of Fig. 4. This is consistent with the time-dependent behaviors of charge and phonon (Fig. 1) and also with experimental observation.[9,10] In the experiment,[9] the weight suppression of $D^+D^+ \rightarrow D^{2+}D^0$ was found not only in PIIMT but also in thermally induced insulator-metal transition (TIIMT) from the LT ($T < T_C$) to the HT phase ($T > T_C$). According to Fig. 4, as A_{ex} increases, both CT1 and CT2 are suppressed and an appreciable weight is developed in the low-energy range ~0.4. However, the Drude-type low-

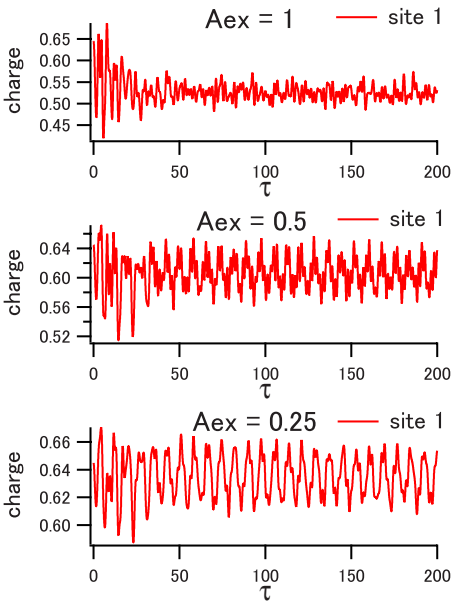

FIG. 3. (Color online) Nonadiabatic-adiabatic changes in the dynamics of charge density at the site 1 with respect to A_{ex}. $\omega_{ex}=1.5$ and $\tau_{ex}=30$ are used.

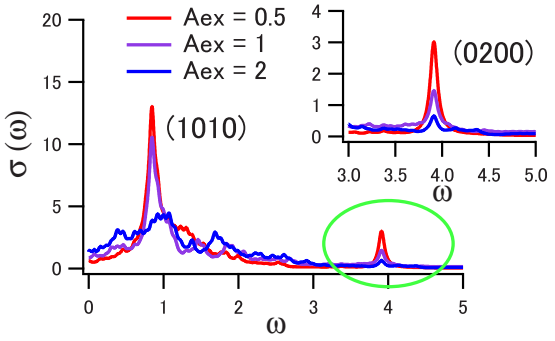

FIG. 4. (Color online) Optical conductivity $\sigma(\omega)$ with respect to the field strength A_{ex}. $\omega_{ex}=1.5$ and $\tau_{ex}=30$ are used. The inset magnifies the behavior of $\sigma(\omega)$ (belonging to an ellipse). (1010) and (0200) represent excitations from (0110) to (1010), i.e., the CT1 band and from (0110) to (0200), i.e., the CT2 band, respectively.

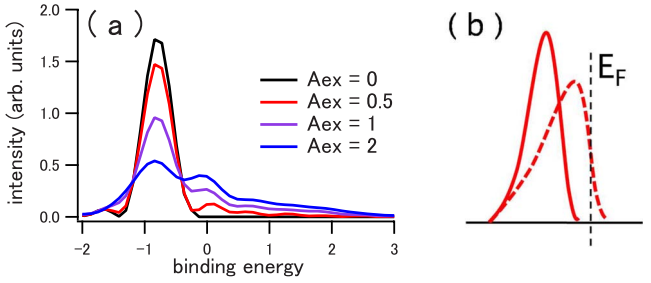

FIG. 5. (Color online) (a) Time-resolved photoemission spectra with respect to the field strength A_{ex}. All spectra are taken at $\tau=50$. $\omega_{ex}=1.5$ and $\tau_{ex}=30$ are used. (b) Sketch of photoemission spectra showing the transition from the LT ($T<T_C$; solid line) to HT phase ($T>T_C$; dashed line) by thermal fluctuation. E_F is the Fermi level.

energy feature is not clearly shown in the figure. This has been in fact experimentally observed and pointed out to differ from TIIMT by Onda *et al.*[10] However, no direct evidence has been found to support their proposal regarding the nonequilibrium (1010) charge-disproportionate state.

C. Time-resolved photoemission

TRPES would probably be the most direct way to observe what happens to the electronic structure after photoexcitation.[24] Theoretical calculations for TRPES are in fact rare due to a lack of the established formalism. However, the present many-body time-dependent approach has merit.[7] We extend our model Hamiltonian $\mathcal{H}$ to include photoemission terms and obtain

$$\mathcal{H}=\mathcal{H}_0+\mathcal{V}(\tau)+\sum_{\mathbf{k}}\varepsilon_{\mathbf{k}}c^{\dagger}_{\mathbf{k}\sigma}c_{\mathbf{k}\sigma}+\mathcal{V}_{\mathrm{pes}}(\tau-\tau_{\mathrm{ex}}),$$

$$\mathcal{V}_{\mathrm{pes}}(\tau)=A_{\mathrm{pes}}\sum_{\mathbf{k}i\sigma}c^{\dagger}_{\mathbf{k}\sigma}c_{i\sigma}e^{i\omega_{\mathrm{pes}}\tau}\Theta(\tau)+\mathrm{H.c.}, \quad (3)$$

where $c^{\dagger}_{\mathbf{k}\sigma}(c_{\mathbf{k}\sigma})$ is the photoelectron[25] with kinetic energy $\varepsilon_{\mathbf{k}}=\mathbf{k}^2/2$. ω_{pes} and A_{pes} are the energy and strength of the photon source adopted for the photoemission. It is now necessary to extend the Hilbert space to include the degree of freedom of the photoelectron. Accordingly, the quantum state of the whole system $|\Psi(\tau)\rangle$ is given by $|\Psi(\tau)\rangle=\Sigma_{\{l,n^{\alpha},n^{\beta}\}}C_{\{l,n^{\alpha},n^{\beta}\}}(\tau)|\{l,n^{\alpha},n^{\beta}\}\rangle+\Sigma_{\mathbf{k}\sigma}\Sigma_{\{l,n^{\alpha},n^{\beta}\}}C^{\mathbf{k}\sigma}_{\{l,n^{\alpha},n^{\beta}\}}(\tau)|\mathbf{k}\sigma\rangle|\{l,n^{\alpha},n^{\beta}\}\rangle$. $|\mathbf{k}\sigma\rangle$ is the state of the photoelectron. TRPES can be simply obtained as $I(E)=\Sigma_{\sigma}\Sigma_{\{l,n^{\alpha},n^{\beta}\}}|C^{\mathbf{k}\sigma}_{\{l,n^{\alpha},n^{\beta}\}}(\tau)|^2$ from the solution of the time-dependent Schrödinger equation $i\partial/\partial\tau|\Psi(\tau)\rangle=\mathcal{H}|\Psi(\tau)\rangle$ for the limit of $A_{\mathrm{pes}}\to 0$ when $\tau>\tau_{\mathrm{ex}}$. E is the binding energy given by $\varepsilon_{\mathbf{k}}-\omega_{\mathrm{pes}}$.

Figure 5(a) presents the TRPES of the system with respect to the field strength A_{ex} together with the photoemission spectra (PES) for the case without photoexcitation (i.e., $A_{\mathrm{ex}}=0$). $\omega_{\mathrm{pes}}=10$ is used. PES without photoexcitation shows a clear gap at the Fermi level but by switching on the photoexcitation, weights of the TRPES spread above the Fermi level. Clearly, the metallic nature strengthens as A_{ex} increases, which is consistent with our previous findings in Figs. 1, 2, and 4. From the TRPES in Fig. 5(a), we can estimate the energy $\mathcal{E}_{\mathrm{charge}}$ absorbed from the external photoexcitation as $\mathcal{E}_{\mathrm{charge}}(A_{\mathrm{ex}})=N/2\times[\int dEEI(E,A_{\mathrm{ex}})-\int dEEI(E,0)]$: $\mathcal{E}_{\mathrm{charge}}(A_{\mathrm{ex}})=0.6$, 1.68, and 2.92 are estimated for $A_{\mathrm{ex}}=0.5$, 1, and 2, respectively.[26] This means that 0.1, 0.28, and 0.49 photons are absorbed per charge (or 0.05, 0.14, and 0.25 per EDO-TTF molecule).

TRPES in Fig. 5(a) illustrate that the energy gap immediately closes in this charge-lattice-coupled system, which is consistent with recent TRPES experiment for $TbTe_3$ showing the melting of CDW.[27] This is different from the Mott insulator. In the Mott insulator, for photoexcitation with $\omega_{\mathrm{ex}}>E_g$ (where E_g is the Mott gap), photoexcited charges transiently reside only at the bottom of the upper Hubbard band so that the gap itself survives.[7] This difference would be due to continuous changes in electronic structures made possible by cooperative interplay between phonons and CO melting. However, in the Mott insulator, there are no degrees of freedom to induce such a continuous change.

It is interesting to discuss differences between PIIMT and TIIMT of the present system. Figure 5(b) gives a sketch of the PES for TIIMT from the LT phase to HT phase. In the sketch, it is understood that only the tail due to the Fermi-Dirac distribution is $\sim k_BT$ (where k_B: the Boltzmann constant) above the Fermi level in the HT phase. In contrast, in Fig. 5(a), there is a wide and appreciable distribution of photoexcited charges above the Fermi level depending on A_{ex}. In thermal equilibrium, the distribution of energy, mode, or number of phonons in the thermal phonon gas is completely governed by temperature. For PIIMT, however, the energy, mode, or number of generated coherent phonons is controlled by the external ultrashort laser pumping. The weight of the TRPES near the Fermi level depending on A_{ex} would be due to the charge response coupled with the coherent phonon.

IV. SUMMARY AND CONCLUSION

In summary, we studied the photoinduced insulator-metal transition of a 1D quarter-filled organic salt by examining the

underlying ultrafast dynamics of charge and phonon within a general nonadiabatic framework. We found that in the early stage to $\tau \sim \tau_{ex}$, there are cooperative onsets of CO melting and coherent phonon oscillation and interplay between the two while later at $\tau \gtrsim \tau_{ex}$, CO melting and coherent phonon oscillation decouple nonadiabatically. Our study of optical conductivity and TRPES at $\tau \gtrsim \tau_{ex}$ reasonably reproduces the recent experimental observations. This provides an evidence for the importance of a nonadiabatic charge-phonon coupling. Finally, we briefly discussed the differences between PIIMT and TIIMT for the present system.

ACKNOWLEDGMENTS

We appreciate constructive discussions with Kenji Yonemitsu and Junichi Inoue. This work was supported by Special Coordination Funds for Promoting Science and Technology and KAKENHI-21740222 from MEXT, Japan.

[1] Y. Tokura, J. Phys. Soc. Jpn. **75**, 011001 (2006); K. Yonemitsu and K. Nasu, Phys. Rep. **465**, 1 (2008), and references therein.
[2] S. Iwai, K. Yamamoto, A. Kashiwazaki, F. Hiramatsu, H. Nakaya, Y. Kawakami, K. Yakushi, H. Okamoto, H. Mori, and Y. Nishio, Phys. Rev. Lett. **98**, 097402 (2007).
[3] C. Kübler, H. Ehrke, R. Huber, R. Lopez, A. Halabica, R. F. Haglund, Jr., and A. Leitenstorfer, Phys. Rev. Lett. **99**, 116401 (2007).
[4] M. Matsubara, Y. Okimoto, T. Ogasawara, Y. Tomioka, H. Okamoto, and Y. Tokura, Phys. Rev. Lett. **99**, 207401 (2007).
[5] M. Imada, A. Fujimori, and Y. Tokura, Rev. Mod. Phys. **70**, 1039 (1998).
[6] S. Iwai, M. Ono, A. Maeda, H. Matsuzaki, H. Kishida, H. Okamoto, and Y. Tokura, Phys. Rev. Lett. **91**, 057401 (2003).
[7] J. D. Lee and J. Inoue, Phys. Rev. B **76**, 205121 (2007).
[8] A. Takahashi, H. Itoh, and M. Aihara, Phys. Rev. B **77**, 205105 (2008).
[9] M. Chollet, L. Guerin, N. Uchida, S. Fukuya, H. Shimoda, T. Ishikawa, K. Matsuda, T. Hasegawa, A. Ota, H. Yamochi, G. Saito, R. Tazaki, S. Adachi, and S. Koshihara, Science **307**, 86 (2005); K. Onda, T. Ishikawa, M. Chollet, X. Shao, H. Yamochi, G. Saito, and S. Koshihara, J. Phys.: Conf. Ser. **21**, 216 (2005).
[10] K. Onda, S. Ogihara, K. Yonemitsu, N. Maeshima, T. Ishikawa, Y. Okimoto, X. Shao, Y. Nakano, H. Yamochi, G. Saito, and S. Koshihara, Phys. Rev. Lett. **101**, 067403 (2008).
[11] K. Ishioka, M. Hase, M. Kitajima, L. Wirtz, A. Rubio, and H. Petek, Phys. Rev. B **77**, 121402(R) (2008).
[12] M. Born and R. Oppenheimer, Ann. Phys. **389**, 457 (1927).
[13] R. T. Clay, S. Mazumdar, and D. K. Campbell, Phys. Rev. B **67**, 115121 (2003).
[14] I. P. Bindloss, Phys. Rev. B **71**, 205113 (2005).
[15] The average numbers of phonons per site would be $\langle b_{i\alpha}^{\dagger} b_{i\alpha} \rangle \approx 0.5$ and $\langle b_{i\beta}^{\dagger} b_{i\beta} \rangle \approx 0.1$ even if they are slightly dependent on A_{ex}. The lattice energy $\mathcal{E}_{lattice}$ absorbed from the photoexcitation would then be $\mathcal{E}_{lattice} \approx 0.08$.
[16] To obtain the known ground state [i.e., (0110) state], in addition to $\mathcal{H}_0$, we have actually considered the infinitesimal on-site energy term that breaks the translational symmetry of $\mathcal{H}_0$, i.e., $\Sigma_{i\sigma} \varepsilon_i c_{i\sigma}^{\dagger} c_{i\sigma}$, where $\varepsilon_i = +\delta, -\delta, -\delta, +\delta, \ldots (i = 0, 1, 2, 3, \ldots)$ and $\delta/t = 10^{-5}$.
[17] O. Drozdova, K. Yakushi, K. Yamamoto, A. Ota, H. Yamochi, G. Saito, H. Tashiro, and D. B. Tanner, Phys. Rev. B **70**, 075107 (2004).
[18] S. Koshihara, Y. Tokura, T. Mitani, G. Saito, T. Koda, Phys. Rev. B **42**, 6853(R) (1990).
[19] K. Yonemitsu, Phys. Rev. B **73**, 155120 (2006).
[20] H. Matsuzaki, M. Yamashita, and H. Okamoto, J. Phys. Soc. Jpn. **75**, 123701 (2006).
[21] K. Iwano, Phys. Rev. B **70**, 241102(R) (2004).
[22] J. D. Lee and J. Inoue, Phys. Rev. B **73**, 165404 (2006); J. D. Lee, J. Inoue, and M. Hase, Phys. Rev. Lett. **97**, 157405 (2006).
[23] K. Yonemitsu and N. Maeshima, Phys. Rev. B **76**, 075105 (2007).
[24] L. Perfetti, P. A. Loukakos, M. Lisowski, U. Bovensiepen, H. Berger, S. Biermann, P. S. Cornaglia, A. Georges, and M. Wolf, Phys. Rev. Lett. **97**, 067402 (2006); L. Perfetti, P. A. Loukakos, M. Lisowski, U. Bovensiepen, M. Wolf, H. Berger, S. Biermann, and A. Georges, N. J. Phys. **10**, 053019 (2008).
[25] Conceptually, in the present problem, we remove holes through the photoemission process. However, we prefer the term *photoelectron* for convenience and also display spectra according to negative binding energy as for the usual PES. Therefore, the spectra in Fig. 5(a) can be simply understood as being from the quarter-filled electron system.
[26] From Ref. 15, we find $\mathcal{E}_{lattice}/\mathcal{E}_{charge} \approx 0.13$, 0.05, and 0.03 for $A_{ex} = 0.5$, 1, and 2, respectively.
[27] F. Schmitt, P. S. Kirchmann, U. Bovensiepen, R. G. Moore, L. Rettig, M. Krenz, J. H. Chu, N. Ru, L. Perfetti, D. H. Lu, M. Wolf, I. R. Fisher, and Z. X. Shen, Science **321**, 1649 (2008).